On the Experimental Stress Analysis of a Composite Box Girder Bridge

By

Ichiro Konishi, Yoshikazu Yamada and Yuhshi Fukumoto

Department of Civil Engineering

Abstract

Experimental researches on composite box girders have been carried out on several bridges and test models and their structural behaviors are gradually becoming clear. The results of the measured stresses obtained at the Yamasu Bridge built in Kyoto in 1955 and the considerations of these results are described in this report. There is good agreement between the theoretical predictions and the actual behavior.

1. Purpose of Experiment

For the exact understanding of the structural characteristics of the composite box girder bidges there remains many obscure points, especially in the quantitative understanding of the stress distributions due to torsion of the box girder caused by the eccentric loading. Therefore, the main purposes of the present experiments are:

(1) The measurements of the distributions of normal stress and shearing stress due to the symmetric loading.

(2) The measurements of the distributions of normal stress and shearing stress due to the eccentric loading.

2. Details of Experiment

The Yamasu Bridge is a welded single box girder bridge, and is designed and executed without temporary supports during placing of the permanent dead load. The height of web plate varies parabolically having the maximum value at the span center and the cross section of the end of this bridge is shown in Fig. 1.
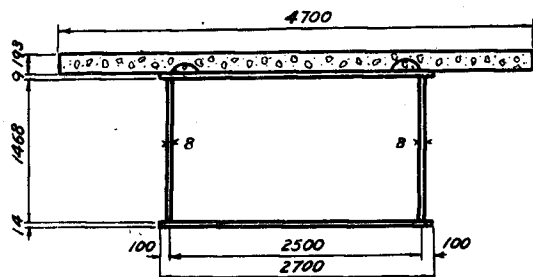

Fig. 1. Cross Section at Span End

The main dimensions are as follows:

|	
Span length	36.300 m
Width of bridge	4.500 m
Steel weight	195 kg/m² .

The main instruments used in these measurements are three strain indicators, five switch boxes for indicator, ASKANIA hand vibrograph and two deflection meters System Tanabe. For test load two trucks, loaded with gravel, are used and each truck weight is 13.0 tons.

To measure the strains at the mid-span cross section these trucks are located near the center of the bridge (experiments No. 1–4), and to measure the strains at the end section these trucks are located near the end of the bridge (experiments No. 5–8).

The location of two trucks is shown in Table 1. The location of strain gages and its marks are shown in Fig. 2.

Table 1.

Experiment No.	Location of Load
No. 1 Symmetric Loading	Two trucks are located side by side and their rear wheels are on the center of the span.
No. 2 Eccentric Loading	One truck is located behind another one on the downstream side and the rear wheel of the former truck is on the center of the span.
No. 3 Symmetric Loading	The loads in No. 2 are removed so as to locate them on the center part of width.
No. 4 Eccentric Loading	The loads in No. 2 are removed so as to locate them symmetrically about the bridge axis.
No. 5 Symmetric Loading	Two trucks are located side by side and their front wheels are on the section A–A one meter apart from the support.
No. 6 Eccentric Loading	One truck is located behind another one on the downstream side and the front wheel of the former truck is on the section A–A.
No. 7 Symmetric Loading	The loads in No. 6 are removed so as to locate them on the center part of width.
No. 8 Eccentric Loading	The loads in No. 6 are removed so as to locate them symmetrically about the bridge axis.
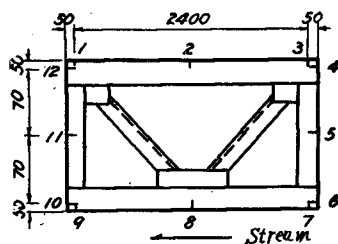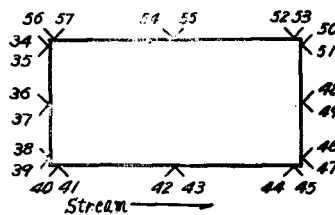
Mid-Span Cross Section   Cross Section A–A

Fig. 2. Strain Gage Locations

3. Measured Results

1) Normal stress σ at main girder

Normal stress σ at the mid-span cross section obtained by the experiments No. 1–4 is shown in Table 2.

2) Shearing stress τ at main girder

Shearing stress τ at the end of the bridge obtained by the experiments No. 5–8 is shown in Table 3. The directions of two wire strain gages to measure the shearing stress are placed at the angle of $\pi/4$ with respect to the bridge axis considering that the principal stresses take these directions at the end of bridge.

Table 2. Normal stress σ, kg/cm², at Span Center

Gage No.	Experiment No.			
	No. 1	No. 2	No. 3	No. 4
1	− 42.0	− 42.0	− 42.0	− 52.5
2	− 21.0	− 42.0	− 42.0	− 31.5
3	− 52.5	− 52.5	− 42.0	− 42.0
4	− 52.5	− 52.5	− 42.0	− 31.5
5	+105.0	+ 84.0	+ 84.0	+105.0
6	+252.0	+210.0	+210.0	+199.5
7	+262.5	+210.0	+210.0	+220.5
8	+252.0	+210.0	+210.0	+210.0
9	+263.0	+210.0	+231.0	+220.5
10	+252.0	+210.0	+210.0	+199.5
11	+105.0	+ 84.0	+ 84.0	+ 73.5
12	− 31.5	− 21.0	− 42.0	− 52.5

Table 3. Shearing Stress τ, kg/cm², at Span End

Gage No.	Experiment No.			
	No. 5	No. 6	No. 7	No. 8
34 35	88.8	45.2	85.7	129.2
36 37	88.8	45.2	76.7	92.9
38 39	68.7	37.5	68.7	113.1
40 41	—	—	—	—
42 43	0	20.2	0	20.2
44 45	60.2	76.7	40.4	16.2
46 47	72.7	105.0	64.6	28.3
48 49	96.9	125.2	84.8	40.4
50 51	88.8	109.0	80.8	36.4
52 53	20.2	24.2	20.2	12.1
54 55	—	—	—	—
56 57	16.2	20.2	20.2	28.3

The maximum shearing stress is calculated from the following equation:

$$\tau_{\max} = \frac{\sigma_1 - \sigma_2}{2} = \frac{E}{2(1+\nu)}(\varepsilon_1 - \varepsilon_2), \qquad (1)$$

where ε_1 and ε_2 are the principal strains.

4. Theoretical Stress Analysis of Main Girder

The theoretical stresses are calculated according to the method given by one of the authors[1].

Fig. 3 shows the standard cross section for the calculation and it is assumed that the cross section is uniform all over the span. In this calculation the ratio of the elastic modulus of
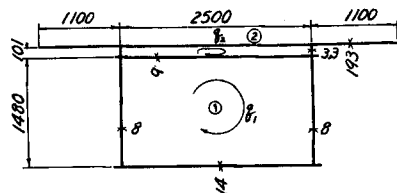

Fig. 3. Standard Cross Section

steel to that of concerete is assmed as $n=6$. With this value, the satisfactory coincidence can be obtained for the calculated and experimental results.

1) Simple torsion

Torsion function $\widetilde{q_i}$ can be defined as

$$\widetilde{q_i} = \frac{q_i}{\frac{d\theta}{dx} G_s}, \qquad (2)$$

where q_i is the shear flow on part i due to simple torsion and G_s is the elastic shearing modulus of steel. So the torsion function $\widetilde{q_i}$ can be calculated as follows.

$$\widetilde{q_1} = 2\frac{c_{22}F_1 + c_{12}F_2}{c_{11}c_{22} - c_{12}^2}, \qquad (3)$$

where c_{11}, c_{12}, c_{22}, F_1 and F_2 are constants which depend on the shape and dimension of the cross section. In this bridge, we have

$$\widetilde{q_1} = 117.46\,\mathrm{cm^2},$$
similarly, $$\widetilde{q_2} = 83.23\,\mathrm{cm^2}.$$

Torsional rigidity K is expressed as

$$K = 4\frac{c_{22}F_1^2 + 2c_{12}F_1F_2 + c_{11}F_2^2}{c_{11}c_{22} - c_{12}^2} G_s + \sum \frac{1}{3} Gbt^3, \qquad (4)$$

and, hence $\qquad K = 7.22808 \times 10^{12}\,\mathrm{kg\text{-}cm^2}.$

2) Shear center

The vertical distance h between the shear center and the fixed point of the cross section can be obtained as follows:

$$h = \frac{M_t}{H} = \frac{\int_F q_h r_c\, ds}{H}, \qquad (5)$$

where q_h is the shear flow due to the horizontal shearing force acting to the shear center S and r_c is the distance between q_h and point C (center of the deck). We obtain $h=21.57\,\mathrm{cm}$ from Eq. (5), that is to say, the shear center is 21.57 cm below the center of the deck.

3) Shear flow due to bending

The cross section being symmetric, the shear flow q_b due to bending is given by Eq. (6),

$$q_b = \frac{Q}{I} \int_0^s \frac{yt}{n}\, ds, \qquad (6)$$

where Q is the shearing force, I is the sectional moment of inertia of the composite girder and $\int_0^s \frac{yt}{n}\, ds$ is the moment with respect to the neutral axis $V\text{--}V$ of the portion

of the cross-sectional area.

The shearing stress τ_b is calculated from the relation, $\tau_b = \dfrac{q_b}{t}$.

4) Bending torsion

The warping function is defined as $W_s = w_s \left/ \dfrac{d\theta}{dx}\right.$, where w_s is the warping occurred in the cross section. The warping function W_s is also shown as follows:

$$W_s = -\int_0^s r_s ds + \int_0^s \frac{\widetilde{q_i} n_g}{t} ds, \qquad (7)$$

where r_s is the distance between the shear center and the center line of the thin-walled sections and $\widetilde{q_i}$ is the torsion function.

The warping function W_s of this bridge is obtained from Eq. (7), and its distribution is shown in Fig. 4.

Bending torsional rigidity $E_s C_w$ can be obtained by using the warping function W_s.

Fig. 4. Warping Function W_s

$$C_w = \int_F \frac{W_s^2 t}{n} ds$$
$$= 15.1843 \times 10^9 \text{ cm}^6. \qquad (8)$$

5) Stresses σ_b and τ_b due to bending

$$\sigma_b = \frac{M}{I} y, \quad \tau_b = \frac{q_b}{t}. \qquad (9)$$

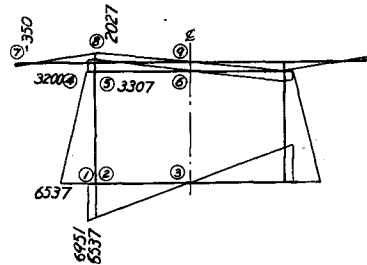The measured stresses in the experiments No. 1, 3, 5 and 7 are shown in Figs. 5(a), 5(c), 7(a) and 7(c) respectively.
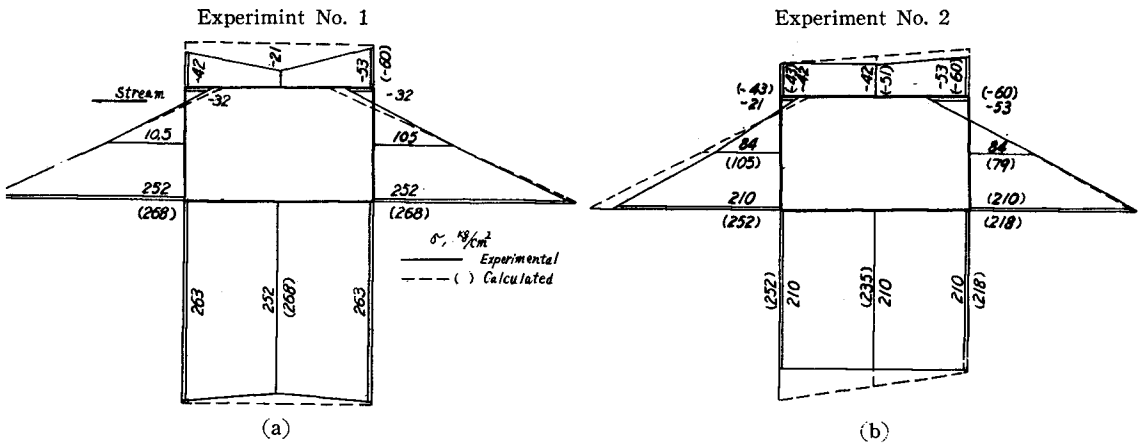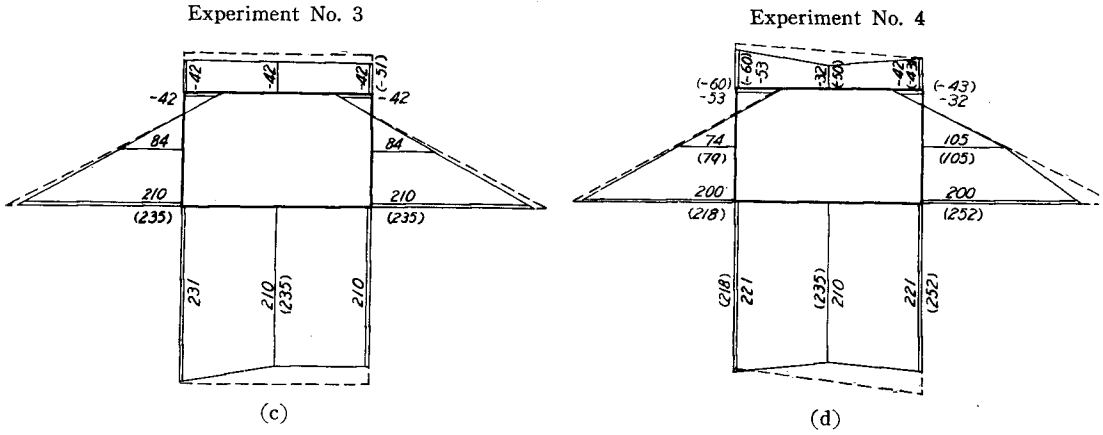

(a)

(b)

Experiment No. 3   Experiment No. 4

(c)   (d)

Fig. 5.   Normal Stress σ at Span Center

6)   Stresses τ_s, τ_w and σ_w due to torsion.

These stresses are calculated from the following equations respectively.

$$\tau_s = \frac{q_s}{t} = \frac{\widetilde{q_s} G_s \dfrac{d\theta}{dx}}{t}. \tag{10}$$

$$\tau_w = -\frac{E_s \dfrac{d^3\theta}{dx^3}}{t}\left[\int_0^s \frac{W_s t}{n}\, ds + S_w\right]. \tag{11}$$

$$\sigma_w = E_s \frac{W_s}{n} \frac{d^2\theta}{dx^2}. \tag{12}$$

Fig. 6.

$\dfrac{d\theta}{dx}$, $\dfrac{d^2\theta}{dx^2}$, and $\dfrac{d^3\theta}{dx^3}$ in the Eqs. (10)$\sim$(12) are obtained from the following equation in the case of a single load (see Fig. 6).

$$\theta(x) = \frac{-\eta \sinh \alpha(l-c)}{\alpha^3 \sinh \alpha l} \sinh \alpha x + \frac{\eta(l-c)}{\alpha^2 l} x + \frac{\eta}{\alpha^3}[\sinh \alpha(x-c) - \alpha(x-c)] \cdot U(x-c), \tag{13}$$

where $\alpha = \sqrt{\dfrac{K}{E_s C_w}} = 1.506 \times 10^{-2}\ \mathrm{cm^{-1}}$

$\eta = P(B-a)/E_s C_w$.

The stresses due to torsion are calculated from Eqs. (10)$\sim$(12) in each experiment as follows:

a)   Experiment No. 2

$$\frac{d^2\theta}{dx^2} = 24.5232 \times 10^{-10},$$

$$\sigma_{w\,\text{max(lower cover plate edge)}} = E_s \frac{W_s}{n} \frac{d^2\theta}{dx^2} = 16.8\ \mathrm{kg/cm^2}.$$

Therefore, normal stress σ is shown as

$$\sigma = \sigma_b + \sigma_w.$$
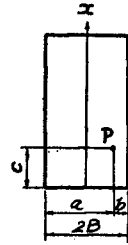
These calculated results are shown in Table 4.

<p align="center">Table 4.   Calculated Stress σ, kg/cm², in Experiment No. 2</p>

Each part at cross section (see Fig. 4)	W_s	σ_w	σ_b	$\sigma = \sigma_b + \sigma_w$	
				Downsteam	Upstrean
2	6,537	± 16.8	234.7	$+251.5$	$+217.9$
3	0	0	234.7	$+234.7$	$+234.7$
5	3,307	± 8.5	-51.2	-42.7	-59.7
6	0	0	-51.2	-51.2	-51.2
web center	4,922	± 12.7	91.8	$+104.5$	$+79.1$

b)   Experiment No. 4

The loading in experiments No. 4 and No. 2 is symmetric about the bridge axis, so we can conclude that the strees distribution in experiment No. 4 is axially symmetric as that of the experiment No. 2.

c)   Experiment No. 6

Value of $\dfrac{d\theta}{dx}$ at the point apart 1 m from the support is equal to 2.7360×10^{-7}.

$$q_1 = \widetilde{q_1} G_s \frac{d\theta}{dx}$$
$$= 117.46 \times 7.88 \times 10^5 \times 2.7360 \times 10^{-7}$$
$$= 25.32 \text{ kg/cm} ,$$
$$\tau_{s1} = \frac{q_1}{t} = \frac{25.32}{0.8} = 31.65 \text{ kg/cm}^2 ,$$

similarly, $\tau_{s2} = \dfrac{q_2}{t} = \dfrac{17.94}{0.8} = 22.43 \text{ kg/cm}^2 .$

d)   Experiment No. 8

$$\frac{d\theta}{dx} = 2.9594 \times 10^{-7} .$$

Same as the experiment No. 6,

$$q_{s1} = 27.39 \text{ kg/cm}, \quad \tau_{s1} = 34.23 \text{ kg/cm}^2 ,$$
$$q_{s2} = 19.41 \text{ kg/cm}, \quad \tau_{s2} = 24.26 \text{ kg/cm}^2 .$$

Therefore, shearing stress τ is shown as
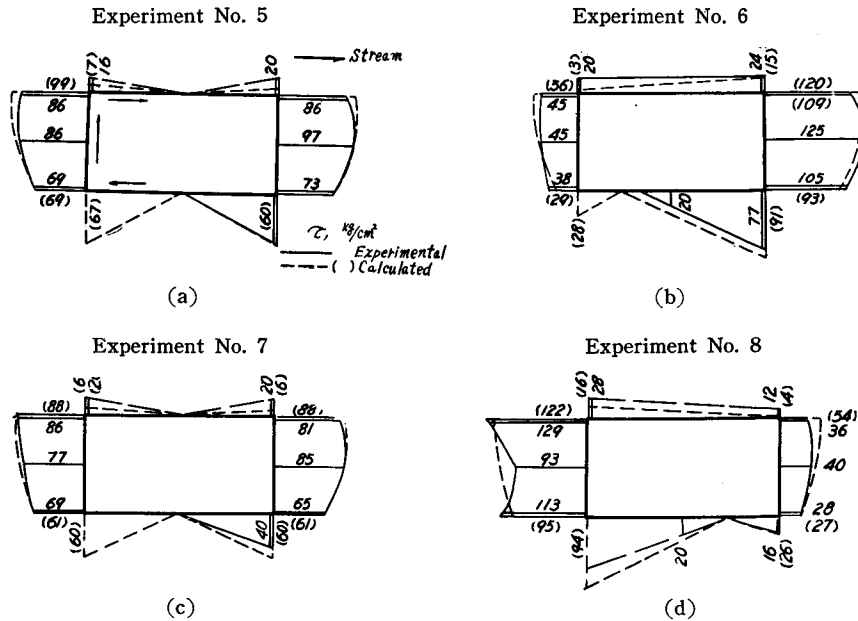
$$\tau = \tau_b + \tau_s + \tau_w .$$

These calculated stresses τ_b, τ_s and τ are shown in Table 5, and in this case τ_w is negligibly small.

Table 5.   Calculated Shearing Stress τ, kg/cm^2

Experiment No.		τ_b	τ_s	$\tau = \tau_b + \tau_s$		
				Upstream	Downstream	
No. 6	q_1	59.71	± 31.65	28.1	91.4	
	q_3	60.89	± 31.65	29.2	92.5	
	q_V	89.08	± 31.65	57.4	120.7	
	q_4	88.09	± 31.65	56.4	119.7	
	q_6	6.02	± 9.22	-3.2	15.2	
No. 8	q_1	59.71	± 34.23	93.9	25.5	
	q_3	60.89	± 34.23	95.1	26.7	
	q_V	89.08	± 34.23	123.3	54.9	
	q_4	88.09	± 34.23	122.3	53.9	
	q_6	6.02	± 10.00	16.0	4.0	
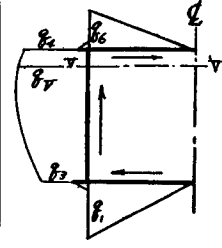
The comparision between the calculated stresses, σ and τ, with the measured values are shown in Figs. 5(a)~5(d) and 7(a)~7(d).

Experiment No. 5

(a)

Experiment No. 6

(b)

Experiment No. 7

(c)

Experiment No. 8

(d)

Fig. 7.   Shearing Stress τ at Span End

5.   Consideration on Experimental Results

1)   Normal stress σ at main girder

a)   The ratios of the measured stresses to the calculated stresses at the center cross section are in case of $n=6$,

88% at the upper cover plate and

93% at the lower cover plate.

In case of $n=10$, those ratios are about 70%. So $n=6$ can be satisfactorily applied to such a composite girder.

b) From the results of calculation, we can obtain that in the experiments No. 2 and No. 4, the proportion of stress σ_w due to the bending torsion to stress σ_b is 7.5% at the lower cover plate and 16.6% at the upper cover plate. From the measured stress distribution we can see that there is little influence of σ_w at the lower cover plate, but there is some influence of σ_w at the upper cover plate, i.e., about 20% to σ_b. There is also the effect of bending torsion at the web plate and its tendency coincides well with that of calculated.

c) There is very little influence of the bending torsion at the lower cover plate where the largest stress occurs.

2) Shearing stress τ at main girder

a) In the experiments No. 5 and No. 7, the measured stresses coincide well with the calculated stresses as shown in Figs. 7(a) and 7(c).

From the results of calculation, we can obtain the following results.

b) Shearing stresses τ_s due to torsion are 32 kg/cm^2 in the experiment No. 6 and 34 kg/cm^2 in the experiment No. 8 and τ_s at the neutral axis is 36% of the shearing stress τ_b, and at the web plate is 36~52% of the shearing stress τ_b. Therefore, the influence of the shearing stress τ_s is comparatively large.

c) The shearing stress τ_w due to bending torsion is negligibly small in this bridge.

6. Conclusion

The results and considerations of the present experiments are described in the previous sections.

The main conclusions obtained in this bridge are as follows:

1) We can use the whole cross section with sufficient accuracy for the calculation of stresses.

2) Composition of the concrete slab to the steel girder for live load is effective and the value $n=6$ is adequate for the load applied in the present experiments.

3) Influence of the bending torsion is negligibly small.

4) Influence of the simple torsion is the most remarkable. Therefore, the above method in which the influence of torsion is considered has to be used to calculate the shearing stress.

5) The result of the measurement of stresses proved good validity of the theoretical formulae used in this report.

6) The experimental results of the deflection are abbriviated in this report, how-ever the experimental values of the deflection are coincided well with the theoretical values, and the ratios of those two values are about 98~100%.

7) Concerning the dynamic deflections the maximum impact factors of the bridge are about 80% when one truck run over the bridge and about 30% when two trucks run at the same time. The latter value is nearly equal to the value used in the design sheet of this bridge.

8) The vibrational characteristics of this bridge are also abbriviated in this report, however the following values are obtained.

Fundamental period of vibration

$$T = 0.368 \text{ sec} \text{ (experimental value)}$$
$$T = 0.363 \text{ sec} \text{ (theoretical value)}.$$

Logarithmic decrement of vibration

$$\delta = 0.066.$$

Reference

1) I. Konishi, S. Komatsu and M. Ohashi; Stress Analysis and Calculation for Design of Composite Box Girder, Trans. of Japan Soc. of Civ. Eng., No. 25, 1955.